

Time-resolved small-angle x-ray-scattering study of ordering kinetics in diblock styrene-butadiene

M. A. Singh

Department of Physics, Queen's University, Kingston, Ontario, Canada K7L 3N6

C. R. Harkless

XonTech Inc., Van Nuys, California 91406

S. E. Nagler

Department of Physics, University of Florida, Gainesville, Florida 32611

R. F. Shannon, Jr. and S. S. Ghosh

Department of Physics, Queen's University, Kingston, Ontario, Canada K7L 3N6

(Received 5 August 1992)

A detailed study of the kinetics of phase transformations of the diblock copolymer, styrene-butadiene, is reported. The technique of *in situ* time-resolved small-angle x-ray scattering with the use of synchrotron radiation has been used to study the first-order phase transitions of microphase separation and microdomain ordering. These transitions occur following a rapid, thermal quench from the homogeneous, disordered state to temperatures below the transition point. The isothermal ordering process is discussed in the context of classical theories of nucleation and growth. Anomalous temporal oscillations in the ordered-volume fraction are observed following quenches to temperatures just below the ordering transition. These results are reported and qualitatively discussed.

I. INTRODUCTION

The study of first-order phase-transition dynamics in block copolymers poses a fascinating, though still poorly understood, problem in phase-transition studies.^{1,2,3} It is well known that the typical incompatibility of chemically distinct polymer segments of the copolymer molecule leads to an incomplete phase-separation process, termed microphase separation.⁴⁻⁸ The resulting microdomains of one chain type tend to form ordered structures or mesophases within a background of the second chain.^{6,7} Recent experimental work^{9,10} has confirmed the fluctuation-induced first-order nature of the transition to a lamellar structure in symmetric and near-symmetric diblock copolymers. In the case of the asymmetric systems considered here, the two processes of microphase separation and ordering, characterized by conserved and non-conserved order parameters, respectively, can be observed to occur separately in time following a rapid thermal quench of the homogeneous mixed-state system.^{11,12} Block copolymers are therefore unique in combining these two classes of kinetic transitions. Furthermore, the nature of the synthesis process¹³ enables detailed regulation of the molecular structure and size, allowing tailoring of the experimental sample to produce desired morphologies and, in principle, to control the time scale of the kinetic processes. This essential flexibility in the design of multicomponent polymeric alloys is of great significance from a practical point of view. The connectivity introduced by covalent bonding of unlike copolymer segments and the dynamics of interdiffusion in long-chain systems are relatively new factors in the study of nonequilibrium phenomena.

In the study of first-order phase transitions, it has proved useful to apply concepts such as scaling behavior and the existence of universality classes, familiar to the study of critical phenomena.¹⁴ These concepts aid in revealing commonalities among the many diverse types of nonequilibrium phenomena. Much of the current experimental work in this area deals with prototypical metallic alloy materials^{15,16} such as Cu₃Au and NiZr₂. Recent studies of the phase-separation kinetics in polymer blend materials, both experimental^{17,18} and theoretical,^{19,20} have demonstrated that predicted early-time linear growth and late-stage dynamical scaling are observed in long-chain systems. It is therefore appropriate to extend this study to encompass the more complex block copolymer materials, which exhibit both microphase-separation and microdomain-ordering processes.

This paper presents the results of a time-resolved small-angle x-ray-scattering (SAXS) study of the phase transitions observed in solutions of asymmetric, diblock styrene-butadiene (SB) copolymer under rapid-thermal-quench conditions. Preliminary kinetic results have been reported in a previous Letter.¹² Detailed measurements of the equilibrium properties of the SB solutions at varying temperatures have been performed to determine the relevant transition temperatures and construct the phase diagram. These results are reported elsewhere.²¹

In Sec. II of this work, details of the sample-preparation procedure, experimental apparatus, and thermal-quench process are discussed. The results of a series of quench measurements performed with copolymer solutions of varying concentration are presented in Sec. III together with a brief discussion of the method of parametrization employed in separating out the relevant

components of the scattering profile. This has been discussed in greater detail in reports of the copolymer equilibrium properties.²¹ The time-dependent properties of the isothermal, intermediate-stage ordering process are discussed in the context of classical theories of heterogeneous nucleation and growth mechanisms^{22,23} in Sec. IV. It is clear from this treatment that the kinetic data do indeed exhibit a form of scaling in the intermediate-stage ordering process, although no evidence of late-stage domain coarsening behavior is apparent. This method of analysis will be compared to a recently proposed model of nucleation and growth²⁴ based on the observed equilibrium coexistence of ordered and disordered phases.

Finally, the unexpected observation of oscillatory growth in the volume fraction of regions of ordered microdomains following a number of relatively shallow thermal quenches will be commented on in Sec. V. It will be shown that this behavior is not due to external influences such as mechanical vibrations or thermal fluctuations. These unusual effects will be the subject of a more detailed experimental study of the shallow quench regime in the near future.

II. EXPERIMENTAL DATA

The fundamental requirement of the experimental apparatus is the ability to take fast, high-resolution measurements of the scattering profile in the small-angle region. In particular, the data-acquisition rate must be faster than the transition process to enable kinetic measurements. Thus the ability to perform fast thermal quenches is essential. With the polymer samples considered here, interesting ordering kinetics occur on the order of seconds following a rapid change in temperature.¹² In addition, high-resolution scattering profiles are required at diffraction angles characteristic of the relevant features of the sample structure. The relevant range in these experiments is^{11,12} $\sim 0.01\text{--}0.05 \text{ \AA}^{-1}$. Finally, pure, highly monodisperse polymer samples are required as a high degree of polydispersity will tend to result in the formation of poorly defined microdomains, thereby inhibiting the ordering process.²⁵

A. Polymer samples

The method of preparation of the styrene-butadiene (SB) polymer solutions has been discussed previously²¹ and is only outlined here. The SB material was synthesized by Polymer Laboratories, Inc. through the anionic polymerization technique¹³ with a fractional composition of 29.5 wt. % styrene, molecular weight of 5.35×10^4 , and polydispersity of 1.03. The pure polymer was mixed with a selective solvent, *n*-tetradecane (C14), in varying proportions to both vary the butadiene fractional volume and lower the interesting transition temperatures to experimentally accessible values. Complete mixing was ensured by dissolving the SB+C14 solutions in an excess of the nonselective solvent CH_2Cl_2 , which evaporates completely over a period of days. Samples of wt. % polymer 14.15 (SB14), 24.13 (SB24), 31.98 (SB32), and 49.80 (SB50) were prepared in this way. The solutions were very nearly clear with some slight cloudiness

in appearance with viscosity increasing with polymer concentration. The vacuum-tight sample cell for scattering measurements consisted of a copper holder sealed with 2-mil Kapton windows with a specimen thickness of 3 mm. The limited flexibility of the Kapton windows allows for some variation in the sample volume. In fact, significant flexing of the windows was observed as the sample temperature was varied within a range of about 30–200 °C, allowing for as much as a 10–20 % change in volume.

Careful thermal-equilibrium measurements performed to establish the sample-dependent temperatures characteristic²⁶ of the onset of microphase separation (T_d) and microdomain ordering (T_o) have been described elsewhere.²¹ The results of these measurements for the varying polymer-solution concentrations are tabulated in Table I. The ordered structure was observed to be body-centered cubic^{12,21} with possible strain-induced fine structure in the SB14 system. This structure was seen to be clearly reversible upon cooling from high temperatures, indicating negligible sample-degradation effects in the measurements reported here.

B. Time-resolved SAXS

The experiments reported here were performed on the joint IBM/MIT beam line X20C of the National Synchrotron Light Source^{12,27} with an estimated incident flux of $\sim 10^{13}$ photons/s/mm². A W-Si multilayer monochromator²⁸ tuned to 8.05 keV was used to ensure a wide energy bandpass for these measurements. A collimation system designed to mask the straight-through beam with minimal parasitic scattering in the small-angle region was employed. The accessible range of the scattering vector was $7.6 \times 10^{-3}\text{--}1.1 \times 10^{-1} \text{ \AA}^{-1}$ ($0.11^\circ\text{--}1.63^\circ$). Scattering profiles were measured with a 1024-element linear position-sensitive array manufactured by EG&G PAR,^{21,28} which, with a sample-detector distance of 803 mm, has a resolution of 566 channels/deg. Typical data-acquisition rates of 0.5 s/scan with between 2 and 6 scans summed per spectrum yielded excellent statistics (6000 counts/s above a background of 100 counts/s) with better-than-adequate time resolution for observation of the transformation processes of interest.

One major impediment to the measurement of transition kinetics in high-polymer systems is the limited efficiency of the thermal quench. Ideally, the change in temperature should occur on a time scale much shorter than that of the transformation process. In practice, this is extremely difficult to achieve because of the typically poor thermal conductivities of most organic polymers.

The actual sample cell, a $12 \times 3 \times 27 \text{ mm}^3$ Cu block

TABLE I. Measured microphase separation (T_d) and microdomain ordering (T_o) temperatures for varying concentrations of SB+C14 solutions.

	SB14	SB24	SB32	SB50
T_o (°C)	86.0	105.5	116.5	154.0
T_d (°C)	121.5	149.5	161.5	200.0

with a $2 \times 3 \times 5 \text{ mm}^3$ slot, was tightly clamped between two $15 \times 12 \times 25 \text{ mm}^3$ Cu blocks. The Cu blocks are resistively heated using two $3\text{-}\Omega$ Ohmite brand wire-wound resistors embedded in their centers. Rapid cooling is achieved by passing coolant (water and He gas) through the two 3.2-mm-diam channels in each Cu heating block. In a typical thermal quench, the sample is first annealed at some temperature $T > T_d$ and then rapidly cooled by forcing a measured amount of coolant through the cooling channels with a timed pulse of pressurized He gas. The variable parameters in the quenching process are the initial temperature T_i , the amount of coolant, and the duration of the He flow, which is controlled by the action of a solenoid valve interfaced to the host computer (an IBM AT). The quench method developed for these experiments employs a “base-temperature undershoot” mechanism to enhance the rate at which the sample temperature changes. The time constant describing the temperature drop of the Cu base under typical conditions ($T_i \approx 200^\circ\text{C}$, $T_f \approx 140^\circ\text{C}$, $\sim 250 \text{ ml H}_2\text{O}$, 1 s burst of He gas) is about 1 s. An effective time constant τ_s of the sample temperature change, assuming only conductive heat loss through thermal contact with the Cu holder, is defined by the expression

$$\Delta T_S = (T_B - T_S) \frac{\Delta t}{\tau_s}, \quad (1)$$

where T_B = base temperature, T_S = sample temperature, and ΔT_S = sample temperature change in a time Δt . The value of τ_s was experimentally determined to be $\approx 6.6 \text{ s}$ for the polymer solutions studied.

Since the base temperature changes rapidly relative to that of the sample, it can be approximated by a constant T_f for the duration of the sample-temperature changes. This leads to a sigmoidal sample-temperature profile as shown by the dashed line in Fig. 1:

$$T_S(t) = (T_i - T_f) e^{-t/\tau_s} + T_f. \quad (2)$$

With the base-temperature undershoot method, however, the initial burst of coolant lowers the base temperature well below the desired final value T_f (see Fig. 1). The latent heat of the resistors then serves to raise the base temperature to within 1°C of T_f as set by a Micristar temperature controller.²¹ As demonstrated in Fig. 1, this technique leads to a significant reduction in the time required to bring the sample temperature from T_i to T_f when compared to standard methods wherein the base temperature is monotonically lowered to T_f . The amount of coolant required to give a maximum base undershoot without undercooling the sample was determined through trial and error. Further heating effects of the residual latent heat were eliminated using 0.25-s bursts of He(g), resulting in a base-temperature ripple of about $\pm 1.0^\circ\text{C}$ and a sample-temperature peak-to-peak ripple of $\pm 0.3^\circ\text{C}$. The frequency with which the He(g) bursts are applied is reduced as the resistor latent heat is reduced. By a time of typically 60 s following the quench, no further gas bursts were necessary to maintain the final temperature T_f . Thermal quenches of the polymer samples to within 1.0°C of the final temperature T_f

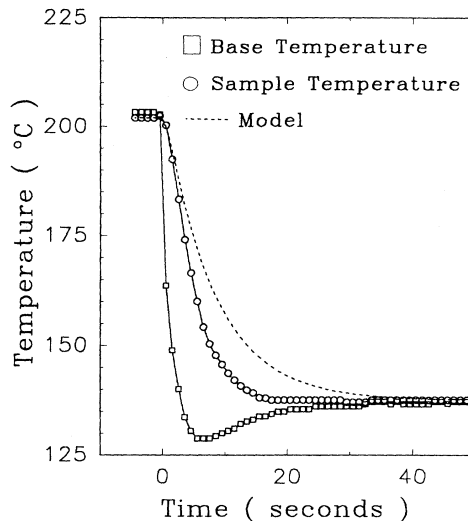


FIG. 1. Temperature profiles for the Cu base and sample temperatures following a typical thermal quench initiated at the zero of time. The model temperature profile is predicted to occur for the standard procedure, wherein the base temperature is monotonically lowered to a final value of $T_f \approx 137^\circ\text{C}$. The sample-temperature profile is predicted with the “base-temperature undershoot” method when the base temperature is initially lowered to $T < T_f$.

without undershoot were typically accomplished in approximately 15 s with T_f maintained with a stability of $\pm 0.3^\circ\text{C}$.

III. EXPERIMENTAL RESULTS

The high intensity of the synchrotron x-ray source enabled acquisition of kinetic data with excellent temporal resolution—typically 1–3 s per spectrum. In all cases polymer samples were annealed at temperatures above the characteristic microphase-separation temperature T_d for at least 15 min before being thermally quenched to the final temperature T_f , as described in the previous section. In each quench experiment, 140 spectra representing sequential time slices of the scattering profile were acquired. Several quenches with varying quench depths ΔT were performed on each sample. The quench depth ΔT is defined relative to the relevant ordering temperature T_o :

$$\Delta T = T_o - T_f. \quad (3)$$

Figure 2 shows the final spectra following quenches for the SB14, SB24, SB32, and SB50 samples for a number of quench depths. The data have been normalized for varying exposure times. The elapsed time of 140 or 420 s has its origin at the time when the sample temperature falls below the microphase-separation temperature T_d . An estimate of the uncertainty in the data can be obtained using Poisson counting statistics.

As discussed in previous works,^{12,21} the observed scattering profile $I(q)$ in the small-angle range of interest, $0.8\text{--}4.5 \times 10^{-2} \text{ \AA}^{-1}$, can be characterized as the sum of three dominant contributions. These are a background

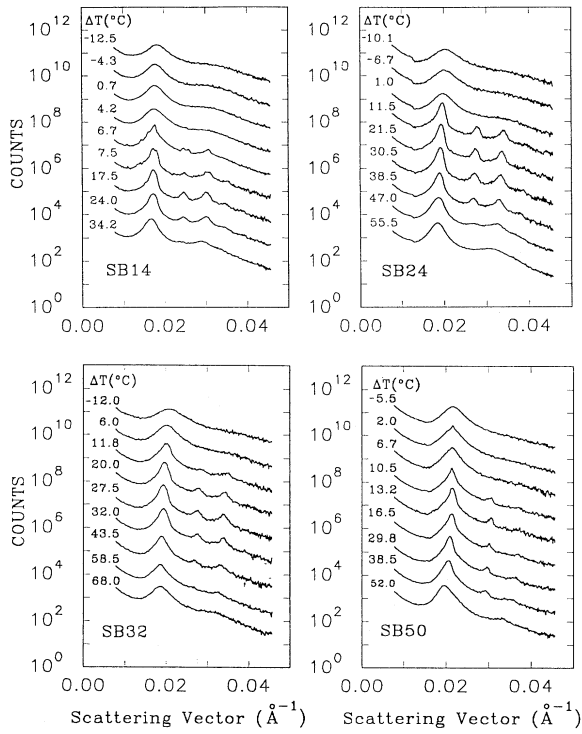


FIG. 2. Stacked, semilog plots of the late-time spectra as a function of quench depth for the four concentrations of SB+C14 studied. It is apparent from the data that microdomain ordering giving rise to Bragg peaks does not occur for quenches to temperatures above T_o or just below T_o .

term $B(q)$, an amorphous scattering contribution $S_a(q)$, and a crystalline scattering contribution $S_c(q)$:

$$I(q) = B(q) + S_a(q) + S_c(q). \quad (4)$$

The background scattering is primarily due to parasitic scattering from window materials and collimating slits. It is measured directly using an empty sample cell and scaled by the ratio of measured intensities so that this term involves no variable parameters.

The amorphous term $S_a(q)$ due to the interacting spherical microdomains is qualitatively similar to the predicted scattering profile of a hard-sphere liquid²⁹ with only two discernible maxima at nonzero q .³⁰ This is well approximated by the expression^{12,21,31}

$$S_a(q) = A_0 \exp \left[\frac{-q^2}{2\sigma_0^2} \right] + A_1 \left[1 + \left[\frac{q-l_1}{\Gamma_1} \right]^2 \right]^{-1} \times A_2 \left[1 + \left[\frac{q-l_2}{\Gamma_2} \right]^2 \right]^{-1}. \quad (5)$$

The variable parameters are the amplitudes A_i , widths σ_0 , Γ_1 , and Γ_2 , and peak positions l_1 and l_2 .

The observable maxima at nonzero q in the amorphous scattering is due to the existence of some local order in

distance can be obtained using the relation³⁰

$$R_{NN} \approx (1.22) \frac{2\pi}{l_1}. \quad (6)$$

Scattering due to the ordered-microdomain structure is represented as the sum of Gaussians^{12,21} with variable amplitudes B_i , widths σ_i , and positions g_i :

$$S_c(q) = \sum_{i=1}^3 B_i \exp \left[-\frac{1}{2} \left[\frac{q-g_i}{\sigma_i} \right]^2 \right]. \quad (7)$$

Figure 3 is representative of the goodness of fit seen with all quench data using this method of parametrization.

It is evident from the data shown in Fig. 2 that no Bragg ordering occurs for quenches with a negative ΔT . This is in accord with observations made in equilibrium studies of these samples.²¹ Similar behavior is observed in shallow quenches, $\Delta T = 4.2^\circ\text{C}$ for SB14 and $\Delta T = 1.0^\circ\text{C}$ for SB24, where T_f is below the measured T_o . The absence of ordering on these time scales can be attributed to the expected reduced driving force for the transformation which is proportional to the free-energy difference between the initial and final states.²³ In the case of the deepest quenches where no Bragg structure is observed (e.g., $\Delta T = 68.0^\circ\text{C}$ for SB32), the absence of microdomain ordering is believed to be due to a reduced thermal activation at the low final temperatures. The possibility of an incomplete microphase separation inhibiting ordering³² can be discounted as the well-defined amorphous peak^{12,21} in the scattering profile indicates a strong interdomain interaction.²⁹ With intermediate, positive ΔT quenches, well-defined Bragg peaks are observed and are consistent with the bcc structure as deter-

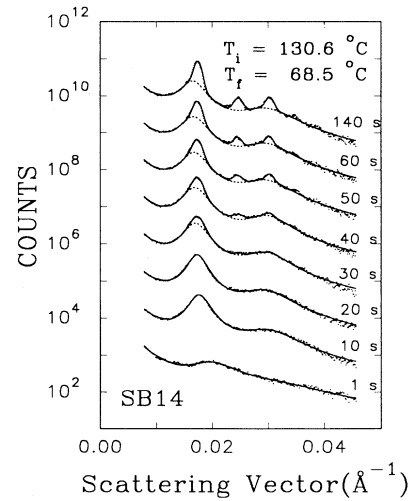


FIG. 3. Stacked, semilog plot of the uncorrected SAXS spectra for the SB14 sample at varying times following a thermal quench of $\Delta T = 17.5^\circ\text{C}$. The data are represented by dots, and the full fit to the data following Eq. (4) is indicated by the solid

mined by both structure-specific fits and volume-fraction calculations.²¹

The discussion of the general kinetic features will refer to the fit parameters of the primary amorphous and Bragg peaks. Figure 3 shows scattering profiles acquired at various times following an intermediate quench of the SB14 sample. At relatively early times, the amorphous scattering profile characteristic of the spherical styrene microdomains in the butadiene-C14 background^{12,21,26} develops rapidly, nearing completion after 20 s. This early-stage process occurs nonisothermally during the quench process, making quantitative analysis of the microphase-separation kinetics difficult. It can be seen that the primary amorphous peak at $\sim 0.2 \text{ \AA}^{-1}$ tends to shift to a lower wave vector while decreasing in width and increasing in amplitude. This behavior is consistent with observations of early-stage phase separation in binary alloys.^{1,26}

The Bragg-peak structure appears at significantly later times following the thermal quench. It can be seen from Fig. 3 that the primary Bragg peak tends to appear at q values close to that of the primary amorphous peak. Given that the first observable Bragg peak for a bcc structure occurs for the [110] set of planes, the relationship between near-neighbor distance and peak position in q space for the ordered structure is similar to that given for the disordered structure in Eq. (6). It is interesting to note that the regular icosahedron is one of three microdomain structures predicted to appear following the microphase separation.⁶ This option is typically discarded as it has fivefold symmetry. Christian²³ discusses the possibility of a liquid or amorphous system being an assembly of molecules with local groupings having symmetries that are inconsistent with the existence of long-range order. These observations suggest that the observed amorphous structure may exhibit the originally predicted⁶ local icosahedral symmetry. This interesting possibility cannot, however, be confirmed without more detailed knowledge of the local groupings of microdomains, but can be considered in the context of Leibler's original mean-field approach.³²

The time development of several features of the scattering profile are summarized in Fig. 4. Errors in the peak-fit parameters are estimated to be on the order of the fluctuation in the curves. The rapidly decreasing primary amorphous peak width indicates an increasing interaction between microdomains as the microphase separation proceeds and interfacial regions become better defined. The observed minimum in amorphous peak width is characteristic of most of the quench data obtained, but is not well understood at present. A detailed analysis of this behavior is complicated by its nonisothermal nature.

The bcc lattice constant is inferred from the fit Bragg-peak position³⁰ and shows a very small ($\sim 0.5\%$) overall decrease with time following the quench. The Bragg-peak width also demonstrates a small overall decrease here ($\sim 15\%$), but this effect was not consistently observed in all the quench data and is small relative to the

Bragg-peak structure is relatively poorly defined. The final leveling off in peak width is not a result of resolution limitations as the instrumental resolution²¹ ($4.4 \times 10^{-4} \text{ \AA}^{-1}$) is significantly narrower than the final peak width.

The normalized intensity of the primary Bragg peak is a function of the peak amplitude, peak width, square of the microdomain form factor, powder averaging factor, and the Debye-Waller factor.²¹ Relative to the changes in peak amplitude, the change in width is negligible. Since the microphase-separation transition is essentially complete at the onset of ordering, the microdomain form factor is assumed to be constant during this process. The very small observable change in Bragg-peak position allows the powder averaging factor to be treated as a constant during the ordering process. Finally, the relatively constant amorphous peak width and sample temperature during ordering indicates a constant Debye-Waller factor.³⁰ The normalized intensity of the primary Bragg peak can therefore be taken to be proportional to the primary Bragg-peak amplitude $B_1(t)$. This quantity is itself proportional to the ordered-volume fraction^{12,21,23} $\xi(t)$, which is a useful measure of the progress of the kinetic process and will be referred to in the following discussion.

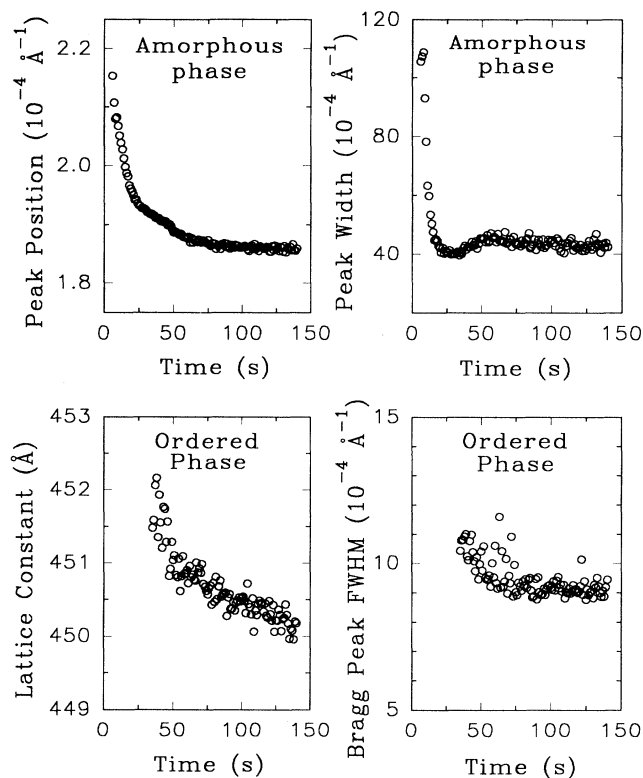


FIG. 4. Graphs of the fit results for the data from the SB24 sample quenched from $T_i = 159.6^\circ\text{C}$ to $T_f = 94.0^\circ\text{C}$: (a) the primary amorphous peak position as a function of time following the quench, (b) the primary amorphous peak width as a function of time following the quench, (c) the bcc lattice constant in-

IV. DISCUSSION OF RESULTS

As discussed in previous work,¹² the Mehl-Johnson-Avrami (MJA) steady-state nucleation theory²³ can be applied to the isothermal microdomain-ordering process observed here. Given an isotropic, thermally activated growth process, the general functional form for the ordered-volume fraction, $\zeta(t)$, as a function of time following a quenching process is predicted²³ to be

$$\zeta(t) = (1 - e^{-bt^n}). \quad (8)$$

The exponent n has a value of 4 for a constant nucleation rate and $n = 1$ for pure one-dimensional growth with no nucleation (site saturation).

The development of the normalized fit amplitude of the first-order Bragg and amorphous peaks of the SB24 sample following a thermal quench to a temperature 11.5°C below the ordering temperature is shown in Fig. 5. Uncertainty in the data is estimated to be on the order of the fluctuations about the smooth curve that can be drawn through the points. It is clear from the figure that the MJA growth law with $n = 1$ and 4 fails, respectively, at early and late times in describing the observed transformation. A best fit of the data to the MJA form over the full range in time yields an intermediate exponent $n = 3.66$, but with significant misfit throughout the measured time range following the quench.

The transition in the MJA exponent n is more clearly demonstrated when considering the quantity²³ $\ln\{\ln[1 - \zeta(t)]^{-1}\}$ as a function of $\ln(t)$ as in Fig. 6. Both $n = 4$ and 1 regimes are clearly evident with the deeper quench depths. With the shallower quench

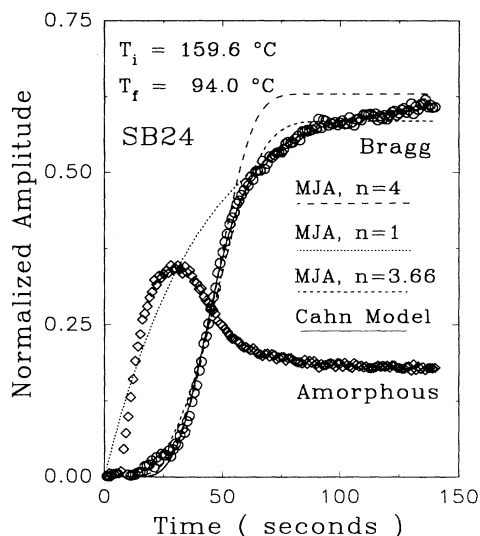


FIG. 5. Normalized amplitudes of the primary Bragg and amorphous peaks as a function of time following the quench for the SB24 sample. Results of the MJA model for the ordered-volume-fraction development are shown for exponents $n = 1$, 3.66, and 4. The resulting fit predicted by the Cahn model (solid line) shows excellent agreement over the full temporal range of the data. The best estimate of the uncertainty in the data is represented by the fluctuation in the points.

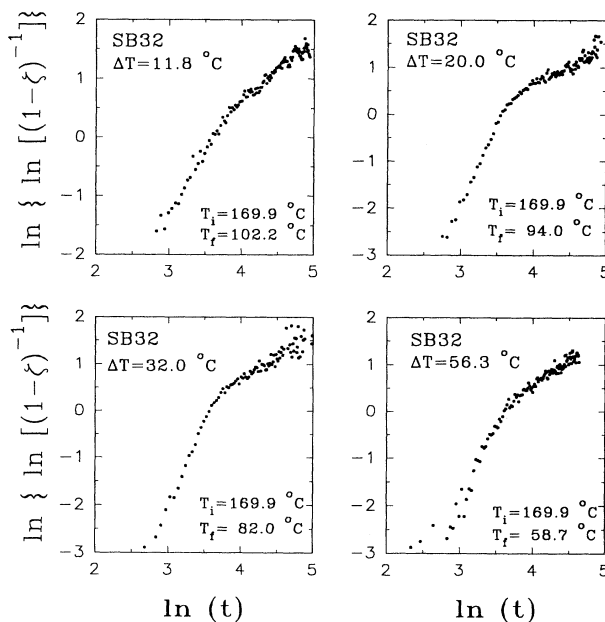


FIG. 6. Plot of the function of the ordered-volume fraction, $\ln\{\ln[1 - \zeta(t)]^{-1}\}$, as a function of $\ln(\text{time})$ for the SB32 sample for four quench depths. The MJA $n = 4$ and 1 regimes are evident at early and late times in the ordering process.

($\Delta T = 11.8^\circ\text{C}$), the crossover occurs at relatively early times and only the $n = 1$ region is visible. The crossover from $n = 4$ to 1 occurring when available nucleation sites are exhausted can be seen to be a function of the quench depth. The polymer samples that have been studied in these measurements are unusual in that both $n = 4$ and 1 limits of the transition process are readily observed.²³

Cahn's classical theory^{22,23} deals specifically with the occurrence of heterogeneous nucleation on two-dimensional defect sites and predicts a crossover in exponent similar to that which is observed. Within this context the time dependence of the ordered-volume fraction has the form

$$\zeta(t) = 1 - \exp[-bf(t - t_0)], \quad (9)$$

where

$$f(t) = \frac{t}{a} \int_0^1 \left\{ 1 - \exp \left[\left[-\frac{\pi}{3} \right] \left[\frac{t}{a} \right]^3 \right] \right\} \times (1 - 3\xi^2 + 2\xi^3) \Big| d\xi,$$

$$a = (I^{ss}\Upsilon^2)^{1/3},$$

$$b = 2V_n \left[\frac{\Upsilon}{I^{ss}} \right]^{1/3}.$$

The variables a and b are related to physical parameters of the system. These are the isotropic growth rate Υ , the steady-state nucleation rate I^{ss} , and the initial volume available for nucleation, V_n . A consideration of Eq. (9) at

late times shows that the ratio a/b is an effective time constant τ for the transformation process in this temporal regime. The variable parameter t_0 arises from the approximation of the time-dependent nucleation rate $I(t)$, with a step function,²³

$$I(t) = \Theta(t - t_0) I^{ss}. \quad (10)$$

The behavior of the transient nucleation rate at very early times in the transformation is not clearly observable as a result of the poor signal-to-noise ratio in the data and the ongoing microdomain-formation process.

The above expression for $\zeta(t)$ reduces to the predicted MJA forms for $n=4$ at early times and $n=1$ at late times. The resulting fit to the data shown in Fig. 5 clearly demonstrates that the observed ordering kinetics can be satisfactorily modeled by this classical theory of heterogeneous nucleation and growth. This approach provides an excellent fit to the bulk of the quench data obtained.

Cahn's expression for the function $\zeta(t)$ suggests the existence of a "master curve" of the form

$$\ln \left\{ \frac{\ln(1-\zeta)^{-1}}{b} \right\} \text{ vs } \ln(t/a). \quad (11)$$

Thus the data can be shown to exhibit a form of scaling behavior through an abscissa translation of $\ln(a)$ and an ordinate translation of $\ln(b)$. Data from 18 different quenching experiments on the four different samples SB14, SB24, SB32, and SB50 are plotted in Fig. 7 according to this expression using the fit parameters a and b . The scatter at low $\ln(t/a)$ is due to the poor signal-to-noise characteristics of the early-time data, while at late times the ordinate term is extremely sensitive to small fluctuations in $\zeta(t)$ resulting from uncertainty in the fit Bragg-peak amplitudes. In spite of the visible scatter at

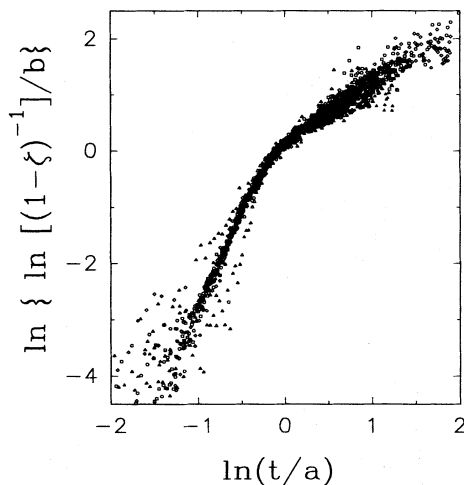


FIG. 7. "Master curve" containing the ordering kinetics for the bulk of the quench data from four concentrations SB14, SB24, SB32, and SB50. The ordinate and coordinate axes are shifted by $\ln(a)$ and $\ln(b)$, where a and b are Cahn-fit parameters.

small and large $\ln(t/a)$, the coincidence of the crossover point in all the data sets is evident.

The effective time constant τ introduced above is inversely proportional to the growth velocity of the ordered domains at late times within the context of the Cahn model. These time constants are plotted as a function of quench depth for the four concentrations of copolymer solution studied in Fig. 8. The results for the SB24 and SB32 solutions clearly exhibit minima at intermediate quench depths, indicating a maximum in the growth velocity as would be expected for a thermally activated growth process. The values of τ determined for the SB14 and SB50 samples are not inconsistent with these observations.

The physical origin of the two-dimensional nucleation sites inherent in Cahn's treatment of the ordering process is, at this time, a matter of some speculation. The likeliest source would appear to be due to anisotropic, solid impurities incorporated into the samples during preparation, as no special precautions were taken to ensure an impurity-free environment. These particles typically exhibit a polyhedral equilibrium shape with planar surfaces that may serve as two-dimensional sites for heterogeneous nucleation. This hypothesis can be most easily tested through observation of the ordering kinetics of samples prepared in a clean environment. Preliminary measurements of the late-time ordering kinetics of clean and "dirty" samples of 25 and 35 wt. % SB+C14 have been performed with an in-house SAXS apparatus. Observable changes in the scattering from clean samples up to 6 h. following thermal quenches to temperatures below T_0 are, indeed, not seen with dirty samples. The measured transition temperatures of the clean and dirty samples agree within estimated uncertainties. These measure-

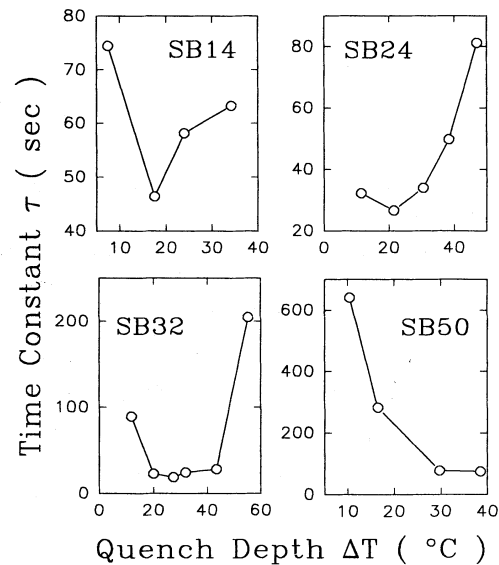


FIG. 8. Predicted time constant of the microdomain-ordering process, τ , as a function of quench depth for the SB14, SB24, SB32, and SB50 polymer solutions. The solid lines are intended as guides to the eye.

ments and the results of a study of the effect of impurities on the early-time kinetics using synchrotron x-ray facilities will be reported in a future publication.

An alternative interpretation of the observed ordering kinetics in these polymer systems was recently proposed by Domany and Nagler.²⁴ They suggest that the observed time dependence is not due to the effects of heterogeneous nucleation, but is, instead, a result of the time independence of the density and equal bulk free energies of the coexisting amorphous and ordered structures. The fundamental assumption of constant density is, perhaps, not well satisfied during these measurements, given the observable flexing of the sample holder Kapton windows during equilibrium measurements (see Sec. II). Furthermore, it should be noted that the assumption of a liquid-like arrangement of microdomains following the microphase separation apparently contradicts the predictions of Leibler's⁶ mean-field theory. The form of the time development of the ordered-volume fraction proposed by Domany and Nagler does, however, provide an adequate fit to these data. A more detailed discussion of the relative merits of these two approaches will therefore be deferred to a future publication dealing with the effects of impurities on the ordering process.

It has already been noted that no significant changes in primary Bragg-peak width was observed in the late stages of the ordering process. The final peak widths are expected to contain contributions from the system resolution, finite size, and strain effects.^{21,28} Hashimoto, Shibayama, and Kawai³³ have noted a similar independence of the Bragg-peak widths as the temperature is varied. They argue that this can be attributed to the dominance of a temperature-independent strain distribution in determining observed widths. Given that even the very low polydispersity of these samples corresponds to a standard deviation of 13% in the distribution of chain lengths, the occurrence of strain dominance in the observed scattering profiles is not unexpected. The broadening due to strain appears to be anisotropic,²¹ and it is difficult to estimate the magnitude of this contribution because of the absence of higher-order Bragg peaks. A lower estimate of 20–40 lattice spacings for the average final ordered domain size can be obtained by ignoring the resolution contribution to the late-stage Bragg-peak widths. The effects of "domain coarsening" are generally observed^{1,34} as a decay of the finite-size contribution to the peak widths when the system is completely ordered. An incomplete ordering process has been consistently observed within the time scales accessible to experiment through equilibrium measurements of coexisting ordered and disordered regions of microdomains²¹ at low temperatures. Given the apparent limited ordering and the presence of a dominant strain contribution to the peak widths, these data cannot be used to discuss domain-coarsening effects.

V. OSCILLATORY GROWTH

In the course of this study of the phase-transition kinetics in diblock copolymer solutions, unexpected observations of oscillatory growth of the Bragg-peak amplitude were made. This anomalous behavior was observed

with several shallow quenches where the final quench temperature was just below the ordering temperature. Oscillatory growth was seen most frequently following shallow quenches of the more concentrated SB50 material and are apparently quasiperiodic in nature. This behavior is demonstrated in Fig. 9.

The oscillatory behavior does not appear to be due to mechanical vibration of the sample cell; nor is it due to fluctuations in the sample temperature which is controlled to within $\pm 0.3^\circ\text{C}$ throughout the time the oscillations are observed. In fact, the oscillations are observed only in the Bragg-peak amplitude and not in the amorphous peak amplitude. When the counting statistics are sufficient, it is also apparent that the pattern of oscillations seen in the primary Bragg-peak amplitude occurs in the secondary and tertiary peaks as well. The possible role played by heat imparted to the sample by the x-ray beam itself should also be considered. Experimental observations of the effects of known x-ray heating in similar materials³² have demonstrated aperiodic, rather than quasiperiodic, fluctuations in the ordered-volume fraction. Also, this behavior is not seen in successive measurements of the equilibrium scattering profile at temperatures near to the transition point. It is most likely, then, that the quasiperiodic fluctuations observed in the Bragg amplitudes are intrinsic to the sample itself and indicate

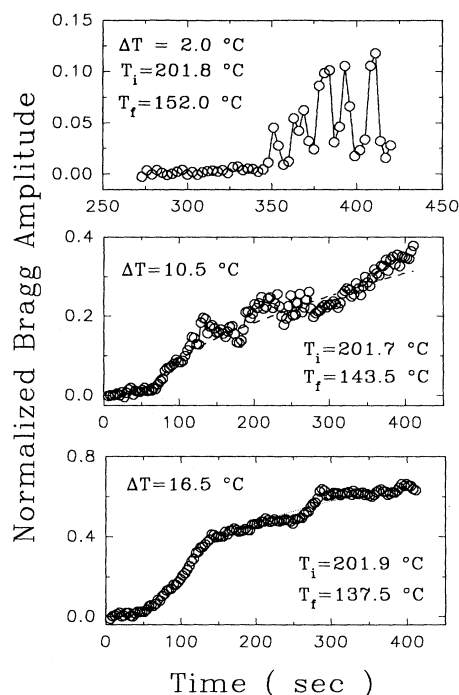


FIG. 9. Graphs of the normalized amplitudes of the primary Bragg-peak fits as a function of time following three thermal quenches of the SB50 sample. The data are represented by open circles, while the solid lines are guides to the eye. The dotted lines in (b) and (c) represent the results of Cahn-model fits to the data. Uncertainty in the values for the peak amplitudes is estimated to be on the order of the fluctuations at early times.

oscillatory growth of the ordered-volume fraction.

Some trends in the nature of the oscillatory data can be tentatively identified on the basis of the limited data available. The quasiperiodic nature cannot be resolved into frequency components with the existing temporal resolution. However, it is clear from Fig. 9 that the dominant frequency increases with decreasing quench depth. The amplitude of oscillation appears to be roughly independent of quench depth. As seen in Fig. 9 with the shallowest quench of $\Delta T = 2.0^\circ\text{C}$, the amplitude of the scattering from the fluctuating ordered-volume fraction is on the order of the total Bragg-peak amplitude.

One obvious interpretation of these observations is that the growth of continuously ordered regions of microdomains is diffusion limited.²³ That is, the latent heat of the ordering transition causes a local change in sample temperature, affecting the growth rate (recalescence). There exists, at present, no data for the latent heat or the thermal conductivities of the polymer solutions in the disordered, microphase-separated, and microdomain-ordered states. However, a crude estimate of the magnitude of the latent heat can be made with the deepest quench depth of 16.5°C based on typical values of the heat capacity of high polymers³⁵ and assuming that recalescence is indeed the source of growth oscillations. The resulting value of about 10^3 kJ/mol appears to be quite high given that the microdomain ordering (crystallization) phenomenon is expected to be only weakly first order.³⁶ A final consideration of the recalescence argument will depend on detailed measurements of the heat capacities and latent heats of transition for these materials.

An alternative interpretation of these data is that the oscillatory growth in the volume fraction of ordered microdomains is due to a finite-size effect arising from a limited number of crystallites in the volume of sample irradiated by the transmitted x-ray beam. In the absence of a true powder average, the fluctuation in Bragg peak may be due simply to the random motion of individual crystallites, although this interpretation seems unlikely given the quasiperiodic nature of the oscillations and the limited mobility of the relatively massive microdomains. This can be most easily checked through variation of the beam spot size in future measurements. With the current spot size at the sample of 0.15×0.50 mm², a sample thickness of 3.0 mm, and an estimated styrene volume fraction of 0.147 for the SB50 material,^{21,28} one would expect to see the scattering from roughly 10^{13} microdomains. Estimates from the width of the Bragg peak at late times suggest an average minimum continuously ordered region of about 20–40 lattice spacings. It therefore seems unlikely, even assuming a relatively large critical radius for nuclei of the ordered phase at shallow quench depths, that the oscillatory behavior is due to a finite-size effect. There is, in fact, an observable tendency toward a decreasing oscillation frequency with increasing quench depth, which also tends to discount this interpretation. However, the enhanced particle mobility resulting from a decrease in critical radius is at least partially offset by the reduced thermal energy available at lower temperatures. Therefore no general conclusions regarding the overall trend in

mobility of the new phase nuclei can be made based on these qualitative arguments.

It may be possible to interpret the observed oscillatory phenomena in the context of recent theories of “growth oscillations” or multiperiodic oscillations in cluster growth velocities.³⁷ If one considers a basic condensation-evaporation mechanism for the nucleation process,³⁸ a stable nucleus results from a dominant condensation rate. In the case of a shallow quench, the driving force for the transition is small and the microdomain-condensation rate will be very near that of the evaporation rate. An oscillation in the growth or condensation velocity, however small, may then lead to an oscillation in the total amount of ordered matter as the dominance of condensation over evaporation is periodically altered. Indeed, the observation of a decreasing oscillation frequency with increasing quench depth tends to support³⁷ the theory of growth oscillations. This interpretation remains purely speculative and will be more carefully studied in a future series of experiments dealing with the effects of shallow thermal quenches.

VI. CONCLUDING REMARKS

The two-stage transformation process involved in the microphase-separation transition in solutions of the asymmetric diblock copolymer, styrene-butadiene, has been clearly observed through time-resolved small-angle x-ray-scattering measurements following a rapid thermal quench. The two temporally separate kinetic processes of microphase separation and ordering are believed to be characterized by conserved and nonconserved order parameters, respectively. The high resolution attained in these measurements enables separation of the early-time microphase-separation and late-time microdomain-ordering processes. At present, the early-time kinetics cannot be evaluated because of its nonisothermal nature.

The time dependence of the ordered-volume fraction cannot be described using the MJA formalism²³ with a single exponent. Instead, a clear crossover in exponent from $n = 4$ and 1 is observed. This behavior can be well characterized by the Cahn model²² for heterogeneous nucleation on two-dimensional defect surfaces. Within this context, the crossover behavior is predicted to occur as a result of saturation of available two-dimensional nucleation sites. The crossover is clearly visible in the majority of these quench experiments. Although it is certainly expected that the process of crystallization in a supercooled liquid will take place through heterogeneous nucleation, the origin of two-dimensional nucleation sites in this system is not entirely clear. An alternative model, based on the apparent equilibrium coexistence of regions of disordered and ordered microdomains, has been suggested by Domany and Nagler,²⁴ which predicts a time development similar to that observed in these measurements without any assumptions regarding the dimensionality of nucleation sites. It is not clear, however, that this model can be applied to these materials. The ordering process suggested by Ishibashi and Takagi³⁹ in dealing with ferroelectric switching also makes no such as-

sumptions. Instead, dimensionality assumptions lie in the structure of the nuclei themselves as is appropriate for strongly anisotropic materials. The proposed growth laws from this model do not, however, account for the observations reported here. These measurements will be repeated with samples containing controlled amounts of impurities to see if, indeed, heterogeneous nucleation is an important factor in determining the transition kinetics.

The existence of a form of scaling behavior is apparent from the superposition of all scaled quench data onto a so-called Cahn master curve.²³ Growth velocities of the ordered-domain interface obtained from the parameters of this model exhibit a maximum at intermediate quench depths as is expected for a thermally activated growth process.

The late-time Bragg peaks arising from regions of continuously ordered styrene microdomains do not show consistent trends in width; the process of domain coarsening cannot be discussed with these measurements. This is clearly not an effect of resolution limitations and is consistent with equilibrium observations,²¹ indicating coexisting regions of ordered and amorphous microdomains at all temperatures and for all experimentally accessible times below the ordering transition point.

Finally, we have observed anomalous oscillations in the time development of the ordered-volume fraction follow-

ing a number of shallow thermal quenches. This phenomenon is not apparently due to undesirable experimental conditions and appears to be intrinsic to the material under study. The possibility of this unusual effect being a manifestation of some form of growth oscillations³⁷ has been suggested. Further experiments in this area with improved resolution in time and quench depth will aid in clarifying the quasiperiodic nature and temperature dependence of these oscillations in order to gain a better understanding of their source.

ACKNOWLEDGMENTS

We would like to thank Ward Ruby and Peter Ma for the excellent technical assistance they provided for this project. Useful discussions with M. N. Butler, D. T. Amm, and T. Zannias are gratefully acknowledged. This research was supported by the U.S. Department of Energy (Office of Basic Energy Sciences) under Grant No. DE-FG05-86ER45280, the Natural Sciences and Engineering Research Council of Canada under Grant No. OGP0046165, and the Ontario Centre for Materials Research under Grant No. QCJ-036. The National Synchrotron Light Source is supported by the U.S. Department of Energy, Division of Material Sciences and Division of Chemical Sciences (Contract No. DE-AC02-76CH00016).

-
- ¹J. D. Gunton, M. San Miguel, and P. S. Sahni, in *Phase Transitions and Critical Phenomena*, edited by C. Domb and J. Lebowitz (Academic, New York, 1983), Vol. 8, p. 267.
- ²K. Kawasaki and K. Sekimoto, *Macromolecules* **22**, 3063 (1989).
- ³E. L. Aero, S. A. Vakulenko, and A. D. Vilesov, *J. Phys. (Paris)* **51**, 2205 (1990).
- ⁴S. Krause, *Macromolecules* **3**, 84 (1970).
- ⁵D. J. Meier, *J. Polym. Sci. C* **26**, 81 (1969).
- ⁶L. Leibler, *Macromolecules* **13**, 1602 (1980).
- ⁷G. H. Fredrickson and E. Helfand, *J. Chem. Phys.* **87**, 697 (1987).
- ⁸G. H. Fredrickson and K. Binder, *J. Chem. Phys.* **91**, 7265 (1989).
- ⁹F. S. Bates, J. H. Rosedale, and G. H. Fredrickson, *J. Chem. Phys.* **92**, 6255 (1990).
- ¹⁰F. S. Bates, J. H. Rosedale, G. H. Fredrickson, and C. J. Glinka, *Phys. Rev. Lett.* **61**, 2229 (1988).
- ¹¹T. Hashimoto, K. Kowsaka, M. Shibayama, and S. Suehiro, *Macromolecules* **19**, 750 (1986).
- ¹²C. R. Harkless, M. A. Singh, S. E. Nagler, G. B. Stephenson, and J. L. Jordan-Sweet, *Phys. Rev. Lett.* **64**, 2285 (1990).
- ¹³H. Hiemenz, *Polymer Chemistry* (Addison-Wesley, New York, 1984).
- ¹⁴K. Binder, *Rep. Prog. Phys.* **50**, 783 (1987).
- ¹⁵S. E. Nagler, R. F. Shannon, Jr., C. R. Harkless, M. A. Singh, and R. M. Nicklow, *Phys. Rev. Lett.* **61**, 718 (1988).
- ¹⁶M. Sutton, Y. S. Yang, J. Mainville, J. L. Jordan-Sweet, K. F. Ludwig, Jr., and G. B. Stephenson, *Phys. Rev. Lett.* **62**, 288 (1989).
- ¹⁷T. Izumitani and T. Hashimoto, *J. Chem. Phys.* **83**, 3694 (1985).
- ¹⁸K. Otake, H. Inomata, Y. Yagi, M. Konno, and S. Saito, *Polym. Commun.* **30**, 203 (1989).
- ¹⁹A. Chakrabarti, R. Toral, J. D. Gunton, and M. Muthukumar, *Phys. Rev. Lett.* **63**, 2072 (1989).
- ²⁰T. E. Schichtel and K. Binder, *Macromolecules* **20**, 1671 (1987).
- ²¹C. R. Harkless, Ph.D. thesis, University of Florida, 1990.
- ²²J. W. Cahn, *Acta Metall.* **4**, 449 (1956).
- ²³J. W. Christian, *The Theory of Transformations in Metals & Alloys*, 2nd ed. (Pergamon, New York, 1981), Pt. I.
- ²⁴E. Domany and S. E. Nagler, *Physica A* **177**, 301 (1991).
- ²⁵T. Hashimoto, M. Shibayama, M. Fujimura, and H. Kawai, *Mem. Fac. Eng. Kyoto Univ.* **14**, 1196 (1981).
- ²⁶T. Hashimoto, K. Kowsaka, M. Shibayama, and H. Kawai, *Macromolecules* **19**, 754 (1986).
- ²⁷G. B. Stephenson, K. F. Ludwig, Jr., J. L. Jordan-Sweet, S. Brauer, J. Mainville, Y. S. Yang, and M. Sutton, *Rev. Sci. Instrum.* **60**, 1537 (1989).
- ²⁸G. B. Stephenson, *Nucl. Instrum. Methods Phys. Res. A* **266**, 477 (1988).
- ²⁹A. Guinier and F. Fournet, *Small Angle Scattering of X-Rays* (Wiley, New York, 1955).
- ³⁰H. P. Klug and L. E. Alexander, *X-Ray Diffraction Procedures for Polycrystalline and Amorphous Materials* (Wiley, New York, 1974).
- ³¹H. E. Stanley, *Introduction to Phase Transitions and Critical Phenomena* (Oxford University Press, New York, 1971).
- ³²M. A. Singh *et al.* (unpublished).

- ³³T. Hashimoto, M. Shibayama, and H. Kawai, *Macromolecules* **16**, 1063 (1983).
- ³⁴S. M. Allen and J. W. Cahn, *Acta Metall.* **27**, 1085 (1979).
- ³⁵*Polymer Handbook*, 2nd ed., edited by J. Brandup and E. H. Immergut (Wiley, New York, 1975).
- ³⁶S. Alexander and J. McTague, *Phys. Rev. Lett.* **41**, 702 (1978).
- ³⁷Z. Cheng, R. Baiod, and R. Savit, *Phys. Rev. A* **35**, 313 (1987).
- ³⁸R. Becker and W. Doring, *Ann. Phys. (N.Y.)* **24**, 719 (1935).
- ³⁹Y. Ishibashi and Y. Takagi, *J. Phys. Soc. Jpn.* **31**, 506 (1971).